Journal of the Brazilian Society of Mechanical Sciences and Engineering (2019) 41:154
https://doi.org/10.1007/s40430-019-1646-6

TECHNICAL PAPER

Collapse of honeycomb cell as a result of buckling or plastic hinges, analytical, numerical and experimental study

Seyed Ali Galehdari[1] · **Mehran Kadkhodayan**[2]

Received: 7 May 2018 / Accepted: 13 February 2019

Abstract
The honeycomb structure collapse during energy absorption and deformation is considered as one of the important subjects for researchers. In this paper, a combined analytical, numerical and experimental analysis on the collapse load of hexagonal aluminum honeycombs due to buckling or plastic collapse of the unit cells under flatwise compressive loading is performed. To analyze the collapse load, some analytical equations are derived for buckling and forming plastic hinges using the frame element. The amounts of these loads are measured for a single-row aluminum honeycomb structure, and the smallest one is selected as collapse load. The results show that the main cause of structure collapse is the formation of plastic hinges. To evaluate the analytical results and to propose a valid numerical simulation method, the quasi-static pressure test is performed. Furthermore, the structure collapse is also simulated by Abaqus software. The maximum difference between the numerical and experimental collapse load is 2.5%. Moreover, the deformed shape of the structure is very similar to the experimental one. The numerical simulation method and the proposed analytical relations can be used to analyze the collapse in other metal honeycomb structures.

Keywords Honeycomb · Plastic collapse · Buckling · Quasi static compression · Finite element analysis

1 Introduction

In addition to having high specific stiffness and strength, honeycomb structures have also superior energy absorption capacity compared to solid plates made of the same material with equal total mass [1]. The mentioned properties have made honeycomb as one of the most promising structures for impact resistance and energy absorption applications, including packaging, automotive, aerospace, etc. Honeycomb structures have been widely used in sandwich panel as a light energy absorber. Sun et al. [2] have investigated the effect of face sheet's thickness and height of honeycomb on energy absorption capacity under quasi-static compression loading using experimental and numerical methods. The thickness of the face sheet has more effect on energy absorption comparing to core geometrical parameters. In another research, Sun et al. [3] have studied the crashworthiness of honeycomb sandwich panels under three point bending load. In this case of loading, the energy absorption was more sensitive to core structural parameters. In this paper, they have derived theoretical equation to predict the peak load and energy absorption. The analytical equations were verified by experimental results. In order to improve crashworthiness of a tube, it can be filled with aluminum foam or honeycomb structures. They have investigated the effect of filling CFRP/aluminum/steel tubes with aluminum foam/honeycomb on crashworthiness parameters. With the increase in the radius of CFRP tubes, both the energy absorption and loading capacities increase. It was noted that in most cases, *SEAs* of the foam-filled CFRP tubes are higher than those of the metallic ones. Also it was that the *SEAs* of CFRP tubes filled with honeycomb are slightly lower than the empty ones [4]. In another paper, the effect of filling a graded thickness tube with functionally graded honeycomb structure on crashworthiness of the structure was studied. Double functionally graded tube has more energy absorption capacity regarding to single functionally graded and

Technical Editor: Paulo de Tarso Rocha de Mendonça, Ph.D.

✉ Seyed Ali Galehdari
ali.galehdari@pmc.iaun.ac.ir

[1] Department of Mechanical Engineering, Najafabad Branch, Islamic Azad University, Najafabad, Iran

[2] Department of Mechanical Engineering, Ferdowsi University of Mashhad, Mashhad, Iran

Published online: 01 March 2019

regular tubes. It was shown that the tubal thickness range has more effect on crashworthiness comparing to honeycomb thickness range [5]. Regarding to the importance of honeycomb structure, the collapse mechanism of these structures should be studied. The honeycomb structure can be used in implants.

Li has verified the feasibility and evaluated the compressive properties of $Ti6Al_4V$ honeycomb-like implants with controlled porosity via electron beam melting process. This process might be a promising method to fabricate orthopedic implants with suitable pore architecture and matched mechanical properties. The response of bare and foam filled honeycomb structure under compression loading has been studied [6]. Foam filled structure can absorb more kinetic energy and apply higher reaction force comparing to bare honeycomb structure [7–11]. Silva and Hunt [12] have studied the buckling of sandwich plates with isotropic and orthotropic cores by analytical method. The analytical model allows separately for bending and shears deformations in the core. Local plastic collapse of thin walled elastic tube was investigated analytically. It was found that the ratio of the maximum mean stress to the critical stress in the columns is linearly related to the breadth to thickness ratio of the walls [13]. Nikravesh and Chung [14] have presented a numerical algorithm to simulate the crash of a vehicle crash using plastic hinge deformation method. Yang and Yu [15] have used elastic perfectly plastic model to predict the plastic behavior of two deformable beams colliding each other. Therefore, the plastic hinge method is applicable to study the plastic collapse of the structures.

Chen et al. [16] studied the competition between in-plane buckling and bending collapses in nano-honeycombs. They investigated the buckling and plastic collapse of the inclined wall of a honeycomb cell. Zhang et al. [17] analyzed the buckling collapse of a honeycomb by large deformation theory to compute the collapse surface for a honeycomb under in-plane biaxial loading. Also, Scarpa et al. [18] presented a combined analytical, numerical and experimental analysis on the compressive strength of a unit cell of hexagonal chiral honeycombs due to buckling under compressive stresses. The mechanical properties of a honeycomb such as failure mechanisms and

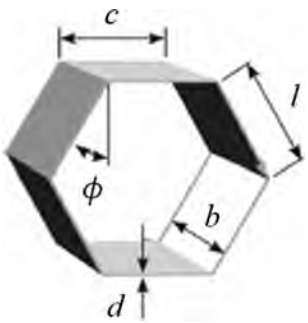

Fig. 1 Honeycomb structure cell

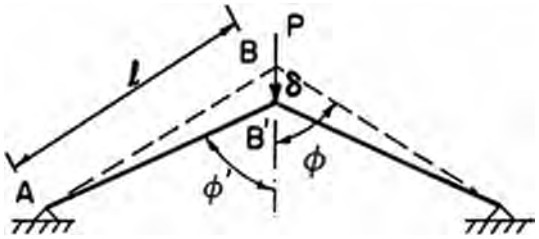

Fig. 2 Inclined beam subjected to a vertical force [39]

deformation modes have been studied by many scientists. [9–28]. They analyzed its in-plane and out-of-plane mechanical behaviors (e.g., buckling or plastic collapse). The post-collapse behavior of a honeycomb material subjected to in-plane compression loading was studied by Karagiozova et al. [29]. They used the limit analysis and the concept of an equivalent structure to show the large plastic deformations of the honeycomb. Sedighi et al. [30] obtained the failure maps of sandwich beams with composite skin and honeycomb core by analytical and experimental methods. Qiao et al. investigated the collapse of a hierarchical honeycomb under in-plane uniaxial loading. They studied the failure modes and collapse stress by finite element simulations under quasi-static loading [31]. Aluminum honeycomb structures have a wide spreading usage in many industries. Their buckling and plastic collapse under low velocity and quasi-static loading have been investigated by numerical and experimental method to find the main reasons for the collapse [32–37].

In this study, the deformation and compression cause of cells are investigated. Analytical equations were derived in order to calculate buckling and plastic collapse load for inclined and horizontal cell wall. In fact, two resembling loads of buckling and plastic collapse are in competition to each other. Cell collapse occurs when the opposite sides of the hexagonal cell become closer or touch each other. In this case, the cells leave their hexagonal shape behind. This collapse may occur because of buckling of the cell sides or the formation of plastic hinges. To analyze the cause of the collapse, the frame element is considered in the analytical and numerical method. In order to validate the analytical and numerical results, the collapse loads of several single-row aluminum honeycomb structures are measured experimentally. A theory to determine

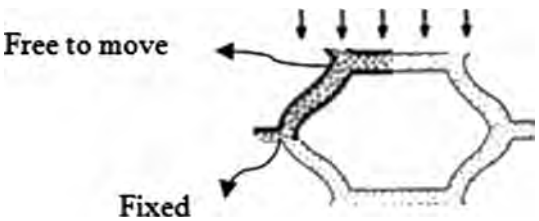

Fig. 3 Boundary conditions of the honeycomb cell side

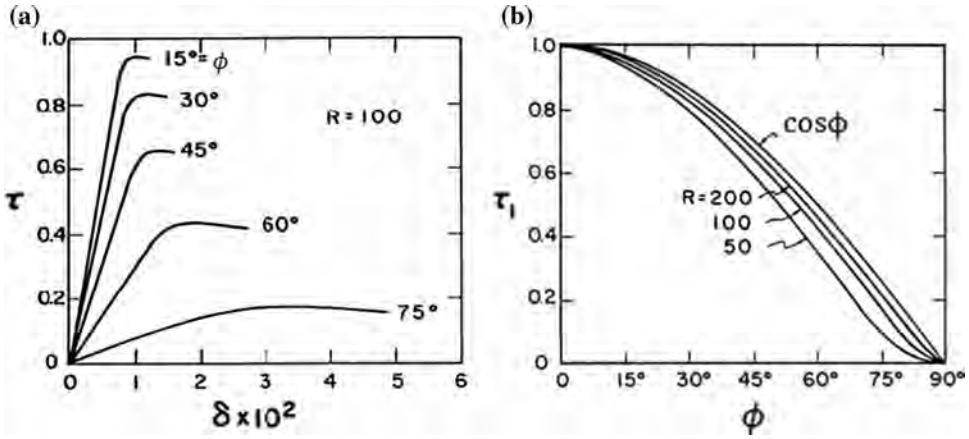

Fig. 4 Variations of **a** τ versus δ, and **b** τ_1 versus ϕ [39]

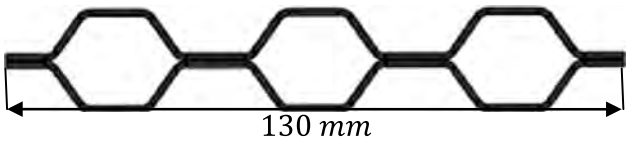

Fig. 5 A single-row honeycomb structure test sample

a competition between the buckling and plastic collapse loads for the inclined and parallel cell walls under uniaxial compression loading is developed. The present theory may be used to design other aluminum honeycomb structures.

2 Collapse analysis of a honeycomb cell

The deformation of a honeycomb structure causes the absorption of applied kinetic energy. This deformation may be a result of forming of plastic hinges or buckling. For more accurate analysis, the deformation of the horizontal and inclined sides of a honeycomb cell is examined and various collapse mechanisms and their loads are compared.

2.1 Study the buckling of the horizontal cell side

Applying axial flat-wise force to a honeycomb cell leads to collapse at the upper and lower contact sides. Then the collapse mechanism which may be buckling or plastic hinge forming can be determined. Friction force may also cause the formation of plastic joints in the middle of the horizontal cell side. Hence, the friction and buckling load of the horizontal side should be calculated. The friction force is equal to $F_f = \mu N$ where N is the normal reaction load, and μ is the coefficient of friction. The magnitude of the normal load is equal to the plastic collapse load. Considering the fixed–fixed boundary condition, the buckling load is calculated using the Euler equation as follows [38]:

$$P_{\mathrm{cri}_1} = \frac{2^2\pi^2 EI}{c^2} \tag{1}$$

In Eq (1), E, I and c are the young modulus, second moment of area and length of the horizontal cell, respectively (Fig. 1.). If the friction load is less than the buckling one, the collapse is due to the formation of plastic hinges rather than buckling.

2.2 Analysis of buckling in the inclined cell side

In this section, buckling in the inclined cell side is studied analytically, considering the frame element. According to Fig. 2, the buckling of an inclined beam subjected to a vertical force is studied.

Table 2 The analytical and numerical buckling loads of the inclined side for various thicknesses

Thickness (mm)	P_{cri_2} (kN) analytical	P_{cri_2} (kN) numerical	Error%
1.6	128.77	147.6	12.7
1.27	66.89	72.41	7.6
1.016	32.31	34.59	6.5

Table 1 Mechanical properties of different thickness of AL-6061-O plate [26]

Thickness (mm)	E (GPa)	n	K (MPa)	e_f (%)	σ_u (MPa)	σ_y (MPa)
1.6	68.28	0.213	202.77	23.76	131.39	51.59
1.27	66.98	0.245	242.66	25.142	141	51.92
1.016	62.5	0.291	220.8	25.168	131	50.7

Table 3 The analytical buckling loads of the horizontal side for various thicknesses

Thickness (mm)	P_{cri_1}(kN) analytical
1.6	116.77
1.27	57.28
1.016	27.36

Table 4 The friction and plastic collapse load of the horizontal side for various thicknesses

Thickness (mm)	P_{cri_3} (N)	F_f (N)
1.6	591	354.6
1.27	444	266.4
1.016	222	133.2

With this regard, the equation of the potential energy of the system consisting of strain energy and the work done by the force P is extracted and using the variation calculation method and the δ operator, the differential equation is obtained [39]. After solving the equation and applying the boundary conditions, the dimensionless buckling force is obtained as [39]

$$\tau = \frac{fR^2}{\beta_0^2} \tag{2}$$

In this equation, $f = \frac{P}{AE}$, $R = \sqrt{\frac{I}{r}}$ where E is the elasticity module, r is the slenderness ratio, I is the second moment of area, and A is the cross section area of the beam. The parameter β_0 depends on the beam's boundary conditions. Based on the above equations, the maximum magnitude on the graph of τ versus δ, τ_1, is equal to the buckling force. The variations of τ versus δ, and τ_1 versus ϕ are shown in Fig. 3. It should be noted that, δ is the vertical displacement of the point B [39]. For this study, the boundary conditions of the honeycomb cell side, one end is fixed, and the other one is free to move in the direction of the applied load, are considered (Fig. 3).

Regarding to Fig. 4, τ_1 can be estimated with the value of cos ϕ. Substituting the buckling force in Eq. (2), this equation can be rewritten as

$$\tau_1 = \frac{fR^2}{\beta_0^2} \geq \cos\phi = \frac{fR^2}{\beta_0^2} \tag{3}$$

Based on the considered boundary conditions, we can use $\beta_0^2 = 4\pi^2$. Therefore, the buckling load of the inclined cell side can be obtained by

$$\cos\phi = \frac{\frac{F}{AE}\frac{l^2A}{I}}{(2\pi)^2} \geq F = P_{cri_2} = \frac{4\pi^2 EI\cos\phi}{l^2} \tag{4}$$

Table 5 Comparison of the buckling and plastic collapse loads for inclined side

Thickness (mm)	P_{cri_2} (kN)	P_{cri_3} (kN)
1.6	128.77	0.591
1.27	66.89	0.444
1.016	32.31	0.222

Table 6 Comparison of the buckling and friction loads for horizontal side

Thickness (mm)	P_{cri_2} (kN)	P_{cri_3} (kN)
1.6	116.77	0.354
1.27	57.28	0.266
1.016	27.36	0.133

Fig. 6 Quasi-static compression test sample

2.3 Analysis of plastic hinge forming

After finding the buckling loads, the load associated with plastic hinges is calculated using the frame element. To obtain this load, the plateau stress of the cell is multiplied by the area affected by the load. The plateau stress equation for the power hardening material model is demonstrated as [40].

$$\sigma_p = \left(\frac{\sigma_u}{n+2}\right)\frac{d^2}{(c + l\sin\phi)(l-d)\sin\phi} \tag{5}$$

In the above equation, σ_u is the ultimate stress of the material and n is the power of the hardening equation. Considering

a honeycomb cell (Fig. 1), the area affected by the load for forming a plastic hinge in the corner of a cell is given by

$$A = b(c + l\sin\phi) \tag{6}$$

According to the above equations, the plastic collapse load of the inclined honeycomb cell, considering the frame element, can be shown as

$$P_{\text{cri}_3} = \sigma_p \times A = \left(\frac{\sigma_u}{n+2}\right)\frac{d^2}{(l-d)\sin\phi}b \tag{7}$$

Putting the cross-sectional area of the entire cell in Eq. (7), the obtained load can be considered for the collapse load of the entire cell. These equations can also be used for the collapse of horizontal and inclined sides. After calculating three forces of P_{cri_1}, P_{cri_2}, and P_{cri_3}, they have to be compared for the cell collapse. These forces are measured experimentally and analytically for single-row aluminum honeycomb structures.

3 Calculation of the buckling and plastic collapse loads

After deriving the equations of buckling and plastic collapse loads, these loads are measured and compared for some honeycomb structures, Fig. 5. For the honeycomb test sample, the geometrical dimensions are as $c = 15$ mm, $l = 12$ mm, $\varphi = 36°$, $b = 28.5$ mm.

This structure is made of Al-6061-O. The mechanical properties for various thicknesses are given in Table 1.

In Table 1, K and n are the coefficient and the power of hardening equation. These coefficients are used for defining the plastic behavior of AL-6061-O for the Abaqus software. The coefficient of friction between the structure and the cross head is taken as 0.6.

3.1 Calculation the buckling load for the horizontal and inclined cell side

Considering the geometric parameters of the cells and Eq. (4), the buckling loads for various thicknesses are calculated and shown in Table 2. To validate the derived analytical equation (Eq. 2), the buckling of the inclined side is simulated by the Abaqus software. The degree of freedom for the end of the beam is fixed, and for the other end of the beam is free to move in the direction of the force. The material properties of Table 1 are used, and the beam element is employed for meshing the inclined cell side. Based on the numerical simulations, the first mode buckling loads of the inclined side for various thicknesses are compared with the analytical loads (Eq. 4), and the results are shown in Table 2.

According to Table 2, considering a maximum difference of 12.7%, the numerical and analytical results retain an appropriate congruence. The buckling loads of the horizontal side with various thicknesses are calculated by Eq. (1) and are shown in Table 3.

The buckling loads obtained for the horizontal and inclined sides are compared with the friction and plastic collapse loads, respectively.

Table 7 compression test results for different thickness

Thickness (mm)	Collapse force (kN)			Average	SD
	Test 1	Test 2	Test 3		
1.016	0.95	1.015	1.065	1.010	0.05766
1.27	1.9305	2.027	2.109	2022	0.08935
1.6	2.620	2.670	2.780	2.690	0.08154

3.2 Calculation of the plastic collapse load of the horizontal and inclined cell side

To calculate the plastic collapse load for the inclined and horizontal sides based on their material properties and geometry, Eq. (7) is used. In this case, the power hardening material model is considered. The friction load of the horizontal side is calculated considering the coefficient of friction and the reaction force (plastic collapse load). The plastic collapse load has been calculated by multiplying the area of horizontal side by plateau stress (Eq. 7). This load and the friction load (F_f) for various thicknesses are demonstrated in Table 4.

The plastic collapse load has been calculated by multiplying the projected area of inclined side by plateau stress (Eq. 7). The loads obtained for buckling and plastic collapse loads for the horizontal and inclined sides are compared. As aforementioned, the plastic collapse and buckling are in competition with each other and the less one is the actual collapse load and

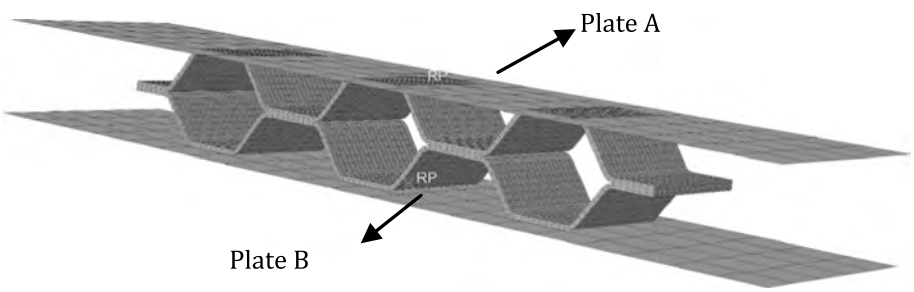

Fig. 7 Finite element model of the single-row honeycomb structure

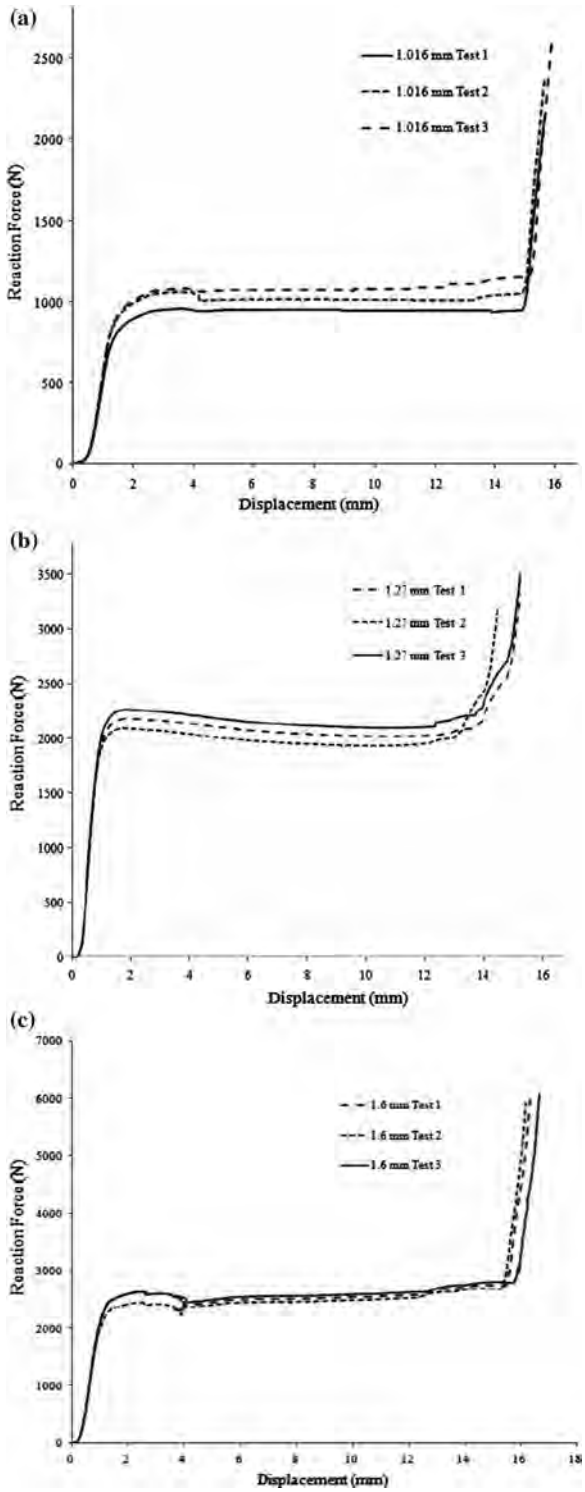

Fig. 8 Load–displacement curves for different thickness

determines the type of collapse (buckling or plastic). Comparison of these loads for the inclined and horizontal sides is shown in Tables 5 and 6, respectively.

According to Tables 5 and 6, the plastic collapse loads are significantly less than the buckling ones for various thicknesses. Therefore, the main collapse cause for inclined and horizontal sides is the formation of plastic hinges.

4 Quasi-static compression test

To determine the accurate collapse load for various thicknesses, the quasi-static compression test is performed on single-row honeycomb samples using Santam tension–compression machine, as shown in Fig. 6. The crosshead speed is 5 mm/min. The reaction force was measured by piezoelectric sensor on the upper crosshead, and the deformation of the structure was measured according to displacement of the upper crosshead. For each thickness, the compression test has been performed on three test samples. Based on the test results, the force–displacement diagram is attained.

4.1 Numerical simulation

To validate the numerical simulation method and analytical equations, experimental results are compared with numerical and analytical ones. Using the measured material properties the plastic behavior of AL-6061O is defined using power hardening model for each thickness individually (Table 1.). It is worth mentioning that due to quasi-static loading, the strain rate of the material is ignored. The 8-node C3D8R cubic and 4-node R3D4 linear elements are used to mesh the honeycomb structure and rigid plates, respectively. The cubic element was used in order to achieve more proper results comparing to experimental ones. The finite element model with the upper and lower rigid plates is shown in Fig. 7.

A penalty contact condition with friction tangential behavior is applied between the bottom element based surface of the structure and the rigid plate, B. In this module based on test condition, the coefficient of friction is considered equal to 0.6. For this quasi-static test, the loading is applied on the structure by plate A. The connection between the different layers of the structure is established using the Tie option. The boundary conditions are defined by constraining the discrete rigid plate, A, to move only in the loading direction and by fixing all the rotational and translational degrees of freedom of the discrete rigid plate, B. Interaction properties are defined using a general contact condition and surface to surface kinematic contact conditions between the top element based surface of the structure and the rigid plate, A. The numerical simulation was performed using Dynamic/Explicit procedure.

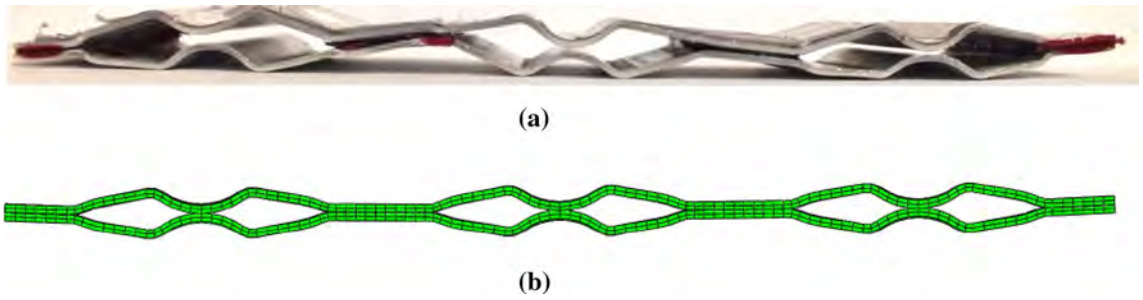

Fig. 9 Deformed shape of the structure with 1.016 mm thickness; **a** experimental test, **b** numerical simulation

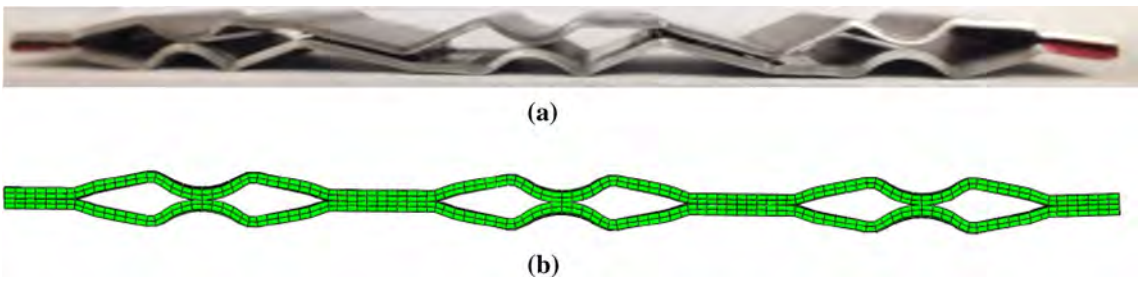

Fig. 10 Deformed shape of the structure with 1.27 mm thickness; **a** experimental test, **b** numerical simulation

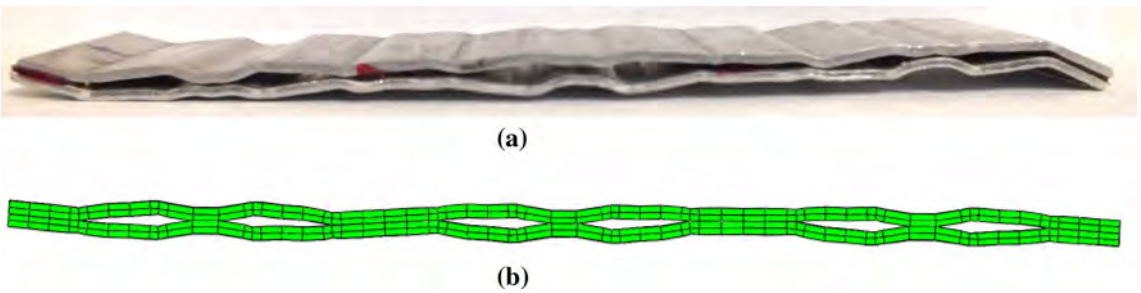

Fig. 11 Deformed shape of the structure with 1.6 mm thickness; **a** experimental test, **b** numerical simulation

Table 8 Experimental and numerical collapse load of the single-layer structure for various thicknesses

Thickness (mm)	Collapse load (kN)		Error%
	Numerical	Experimental	
1.6	2.690	2.626	2.5
1.27	2.022	2.022	0
1.016	1.010	1.010	0

Table 9 Experimental, numerical and analytical collapse load of the inclined cell side for various thicknesses

Thickness (mm)	Collapse load (kN)		Analytical (Eq. 7)
	Numerical	Experimental	
1.6	0.577	0.591	0.591
1.27	0.444	0.444	0.444
1.016	0.222	0.222	0.222

5 Results and discussion

The compression test results of test samples for different thickness are reported in Table 7. Also their load–displacement curves are shown in Fig. 8.

According to Table 7 and Fig. 8, because of low standard deviation, the experimental results for each thickness are reproducible. The average collapse force magnitude is used to compare with numerical and experimental results.

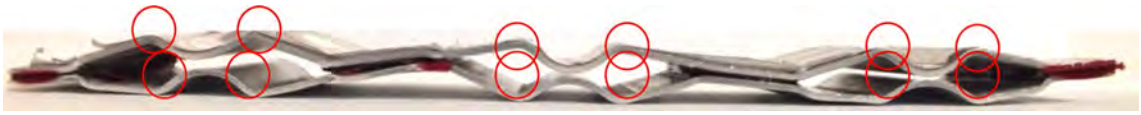

Fig. 12 The formed plastic hinges in the single-layer structure with 1.016 mm thickness

The obtained numerical and experimental deformed shapes of structure due to quasi-static loading for different thicknesses are shown in Figs. 9, 10 and 11.

The magnitude of the collapse loads for quasi-static experimental test and numerical simulation is shown in Table 8.

As Table 8 suggests, the obtained numerical results have good congruence with the experimental ones. The maximum difference between the numerical and experimental results is 2.5%. In addition, according to Figs. 9, 10 and 11, the numerical deformed shapes of the structure are similar to the experimental shapes. Thus, the numerical simulation method and the utilized parameters are validated.

The magnitude of the experimental collapse loads is measured for the entire single-layer structure. It is noteworthy that the plateau stress is equal for each cell side and the whole structure. The collapse force is calculated by multiplying the plateau stress by the cross section of each cell or cell side. According to Table 8, comparisons between the analytical, numerical, and experimental collapse loads for the inclined cell side with various thicknesses are shown in Table 9.

Regarding to Table 8, the obtained loads with different methods retain an appropriate agreement. Therefore, the formation of the plastic hinges (plastic collapse) is confirmed as the main cause of structure collapse. The formed plastic hinges in the test sample are shown in Fig. 12.

6 Conclusion

In this study, the collapse load of a metal honeycomb structures was investigated. Structure collapse may occur as a result of buckling or formation of plastic hinges. After deriving the analytical equations for each collapse loads, their values for an aluminum sample were calculated. By comparing these loads, the plastic hinge formation load was identified as the main cause of collapse. To evaluate the calculated loads and to investigate cause of collapse, quasi-static compression test along with the numerical simulation was performed on several single-layer honeycomb structures. With this regard, the collapse loads were measured by experimental and numerical method. The maximum difference between the numerical and experimental results was 2.5%. Hence, the main reason of the structure collapse (plastic hinge forming) predicted by analytical method was confirmed using experimental and the numerical method. The utilized numerical method is applicable for analyzing the collapse cause of similar honeycomb structures. The derived analytical equations can be utilized for upper and lower rows of a honeycomb structure or for all rows of a graded honeycomb structure.

References

1. Xue ZY, Hutchinson JW (2004) A comparative study of impulse-resistant metal sandwich plates. Int J Impact Eng 30(10):1283–1305
2. Sun G, Chen D, Huo X, Zheng G, Li Q (2018) Experimental and numerical studies on indentation and perforation characteristics of honeycomb sandwich panels. Compos Struct 184:110–124
3. Sun G, Li S, Liu Q, Li G, Li Q (2016) Experimental study on crashworthiness of empty/aluminum foam/honeycomb-filled CFRP tubes. Compos Struct 152:969–993
4. Sun G, Jiang H, Fang J, Li G, Li Q (2016) Crashworthiness of vertex based hierarchical honeycombs in out-of-plane impact. Mater Des 110:705–719
5. Zhu G, Li S, Sun G, Li G, Li Q (2016) On design of graded honeycomb filler and tubal wall thickness for multiple load cases. Thin-Walled Struct 109:377–389
6. Li X, Wang C, Zhang W, Li W (2010) Fabrication and compressive properties of Ti6Al4 V implant with honeycomb like structure for biomedical applications. Rapid Prototyp J 16(1):44–49
7. Jhaver R, Tippur H (2010) Characterization and modeling of compression behavior of syntactic foam-filled honeycombs. J Reinf Plast Compos 29:3185–3196
8. Mozafari H, Khatami S (2010) Molatefi, out of plane crushing and local stiffness determination of proposed foam filled sandwich panel for Korean Tilting Train express—numerical study. Mater Des 31:1216–1230
9. Alavi Nia A, Sadeghi MZ (2013) An experimental investigation on the effect of strain rate on the behaviour of bare and foam-filled aluminum honeycombs. Mater Des 52:748–756
10. Alavi Nia A, Sadeghi MZ (2016) The effects of foam filling on compressive response of hexagonal cell aluminum honeycombs under axial loading-experimental study. Mater Des 66:400–411
11. Mozafari H, Khatami S, Molatefi H, Crupi V, Epasto G, Guglielmino E (2016) Finite element analysis of foam-filled honeycomb structures under impact loading and crashworthiness design. Int J Crashworthiness 21(2):148–160
12. Silva LS, Hunt GW (2007) Interactive buckling in sandwich structures with core orthotropy. Mech Based Des Struct Mach 18(3):353–372
13. Smith TRG, Sridharan S (2007) The local collapse of elastic thin walled columns. Mech Based Des Struct Mach 8(4):471–489
14. Nikravesh PE, Chung IS (2007) Structural collapse and vehicular crash simulation using a plastic hinge technique. Mech Based Des Struct Mach 12(3):371–400

15. Yang JL, Yu TX (2007) Dynamic plastic behavior of a free-rotating hinged beam striking a cantilever beam. Mech Based Des Struct Mach 29(3):391–409
16. Chen Q, Pugno NM (2012) Competition between in-plane buckling and bending collapses in nano-honeycombs. Lett J Explor Front Phys 98(16005):1–5
17. Zhang J, Ashby MF (1992) Buckling of Honeycombs under in-plane biaxial stresses. Int J Mech Sci 34(6):491–509
18. Scarpa F, Blain S, Lew T, Perrott D, Ruzzene M, Yates JR (2007) Elastic buckling of hexagonal chiral cell honeycombs. Compos A 38:280–289
19. Warren WE, Kraynik AM (1987) Foam mechanics: the linear elastic response of two dimensional spatially periodic cellular materials. Mech Mater 6:27–37
20. Papka SD, Kyriakides S (1994) In-plane compressive response and crushing of honeycombs. J Mech Phys Solids 42:1499–1532
21. Papka SD, Kyriakides S (1998) Experiments and full-scale numerical simulations of in-plane crushing of a honeycombs. Acta Mater 46:2765–2776
22. Papka SD, Kyriakides S (1998) Biaxial crushing of honeycombs. Part I: experiments. Int J Solids Struct 30:4367–4396
23. Papka SD, Kyriakides S (1998) In-plane biaxial crushing of honeycombs, Part II: analysis. Int J Solids Struct 30:4397–4423
24. Gibson LJ, Ashby MF (1997) Cellular solids: structure and properties, 2nd edn. Cambridge University Press, Cambridge
25. Bhat BT, Wang TG (1990) A comparison of mechanical properties of some foams and honeycombs. J Mater Sci 25:5157–5162
26. Nakamoto H, Adachi T, Araki W (2009) In-plane impact behavior of honeycomb structures randomly filled with rigid inclusions. Int J Impact Eng 36:73–80
27. Ramavath P, Biswas P, Ravi N, Johnson R (2016) Prediction and validation of buckling stress of the ceramic honeycomb cell walls under quasi-static compression. Cogent Eng 3:1–7
28. Wilbert A (2010) On the crushing of honeycomb under axial compression. M.Sc. Thesis, The University of Texas, Texas
29. Karagiozova D, Yu TX (2005) Post-collapse characteristics of ductile circular honeycombs under in-plane compression. Int J Mech Sci 47:570–602
30. Sadighi M, Dehkordi AA, Khodambashi R (2010) Theoretical and experimental study of failure maps of sandwich beams with composite skins and honeycomb core. Amirkabir Mech Eng Technol J 42(1):37–47
31. Qiao J, Chen C (2016) In-plane crushing of a hierarchical honeycomb. Int J Solids Struct 85:57–66
32. Crupi V, Epasto G, Guglielmino E (2012) Collapse modes in aluminium honeycomb sandwich panels under bending and impact loading. Int J Impact Eng 43:6–15
33. Yamazaki K, Fukasaku R, Kitayama S, Furutochi M (2006) Development of cell structure for impact energy absorption with film ruptures. Trans Jpn Soc Mech Eng Ser A72(723):1654–1661
34. Nakamoto H, Adachi T, Higuchi M (2013) Approximate analysis of progressive deformation in honeycomb structures subjected to in-plane loading. Arch Appl Mech 83(3):379–396
35. Wilbert WY, Jang JS, Floccari JF (2011) Buckling and progressive crushing of laterally loaded honeycomb. Int J Solids Struct 48(5):803–816
36. Mohr D, Doyoyo M (2013) Nucleation and propagation of plastic collapse bands in aluminum honeycomb. J Appl Phys 94(4):1–7
37. Chung J, Waas, AM (1999) Collapse, crushing and energy absorption of circular-celled honeycombs, AIAA-1999-1358, AIAA/ASME/ASCE/AHS/ASC structures, structural dynamics, and materials conference and exhibit, Collection of technical papers, vol. 2, (A99–24601 05-39)
38. Timoshenko SP, Gere JM (1985) Theory of elastic stability. McGraw-Hill, New York
39. Chang CH (2005) Mechanics of elastic structures with inclined members. Springer, New York
40. Galehdari SA, Kadkhodayan M, Hadidi-Moud S (2015) Low velocity impact and quasi static in plane loading on a graded honeycomb structure; experimental, analytical and numerical study. Aerosp Sci Technol 47:425–433